

Contributions to the experimental study regarding the influence of the cutting fluid on the grinding process performances

CONSTANTIN BUZATU, ADELA-ELIZA DUMITRASCU
Engineering Technology Department
Transylvania University of Brasov
Brasov, B-dul eroilor 29
ROMANIA

Abstract: In the paper is shown a theoretical study regarding the manner in which the cutting fluid influences the performances of the grinding process. The quantity of heat that results during grinding process is transmitted to the technological elements which influence the thermal deformations of the workpieces and their dimensional accuracy and surface finish. Also, are distinguished experimental data regarding the influence of cutting speed on the temperature in machining zone in the case of different cutting processes.

Key-Words: cutting fluid, temperature, grinding, balance, accuracy, machining zone.

1 Introduction

Grinding is a manufacturing process with tools with undefined geometry. Some authors think that grinding operation can be compared with milling with disc milling cutter considering that an abrasive grain can be as a tooth of milling cutter. But this model has drawbacks in that the abrasive grains have different sizes, clearance and rake angles and are situated at different distances each others.

Also at grinding wheel the characteristics of cutting edges of abrasive grains are changing continuously and as a consequence the temperature which is raised in the contact tool workpiece has a variable range.

Now we will consider a simplified case when an abrasive grain is in contact with the part surface. If the abrasive grain is located at a distance that it doesn't allow to cut it only rubbing the part surface without removing chips.

This represents a first heat source Q_1 . The force on abrasive grain increases and it can be fractured and this is other heat source Q_2 .

2 Heat sources at grinding operation

If the abrasive grain removes chips at the tool part contact are three zones as a heating zone (Fig.1). Zone I is of elastic deformation, zone II is of elastic and plastic deformation and zone III is zone where are removing chips [1].

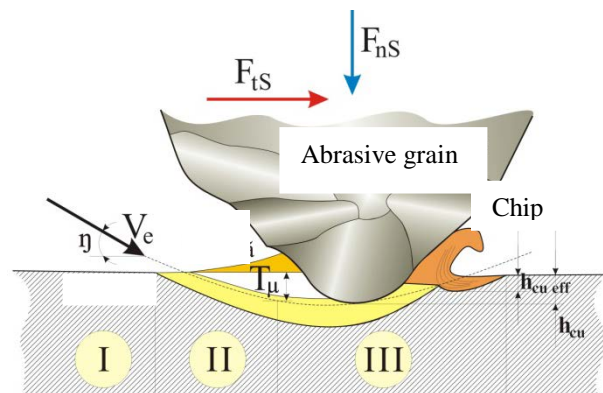


Fig.1 Removal of chips at grinding operation.

The heat in contact zone is generated by transformation of mechanical energy required for chip formation, ploughing and against friction caused by rubbing of the grain along the part surface.

As is shown in Fig.2 we will designate the heat in the contact tool part surface zone by: Q_{ff} the heat at friction, Q_r the heat between rake face and chip, Q_α heat between rake face and part, Q_{det} , heat to remove the chip, Q_{intas} heat caused by friction forces inside the chips.

The total heat quantity (Q_c) in cutting zone can be evaluated as is shown in equation below [2]:

$$Q_c = \sum Q_{g1} + \sum Q_{g2} \quad (1)$$

where: Q_{g1} is the heat produced by an abrasive grain in contact with part surface and Q_{g2} is the heat produced by the abrasive grain which doesn't cut.

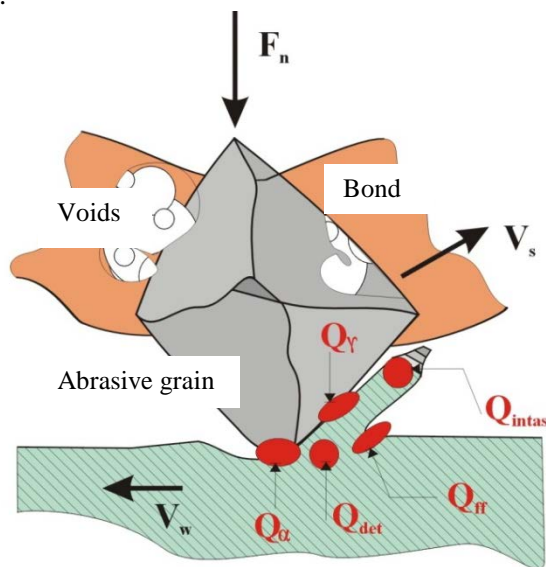


Fig.2. Heat sources at removing chips.

$$\sum Q_{g1} = \sum Q_{ep} + \sum Q_{fg} \quad (2)$$

where: Q_{ep} is the heat generated during the elastic and plastic deformation of part material by the abrasive grain and Q_{fg} is the heat produced by the fracture of abrasive grain.

$$\sum Q_{g2} = \sum Q_I + \sum Q_{II} + \sum Q_{III} \quad (3)$$

where, Q_I , Q_{II} , and Q_{III} are the heat from the zone I, II, and III.

3 Research of the influence of cutting fluid on the grinding performances

Experimental researches regarding the influence of the cutting fluid on grinding operation were made on the flat surface grinding machine. The workpieces were bearing rings that have been processed on the two flat surfaces.

Simultaneous flat surface grinding is a process in which parts are processed simultaneously on both sides by the front face of abrasive wheels (Fig.3).

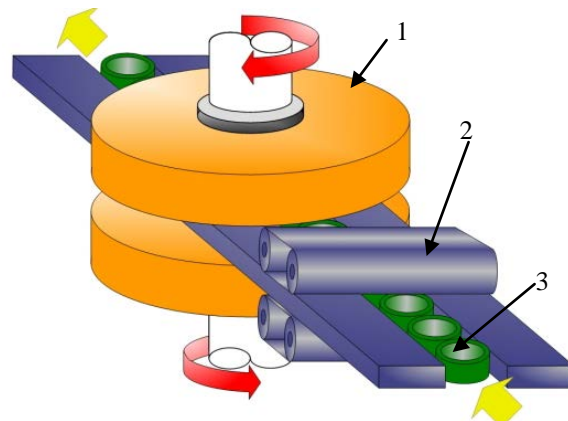


Fig.3 The working principle of simultaneous flat grinding machines.

The workpieces (3) are laterally guided and a system of rollers (2) brings them between two grinding wheels (1). The amount of material removed from the flat parts surfaces depend on the speed of abrasive wheels. During processing abrasive bodies wear out and with it the width of the parts increases. Dimensional corrections are made automatically or manually after parts measurement. The two grinding wheels can rotate in the same or in the opposite direction.

Experimental research showed that the dimensional stability and surface roughness of the machined parts are better if the grinding wheels have opposite direction of rotation.

The methods used for cutting fluid management in the cutting process are:

- a) Two nozzles located at the top of the middle of abrasive bodies (Fig.4);



Fig.4 Penetration of the cutting fluid from the top of the grinding bodies.

The distance between the grinding wheels and parts guided system is about 1 mm, which means that the area of cutting fluid penetration is very small, so the amount of cutting fluid that penetrates the contact area is very small. Cutting fluid delivered by this method is involved in the grinding process only when the parts are in the second half of the abrasive bodies and therefore when the half of the machining allowance has been removed.

b) By 30 mm bore in the center of the abrasive body (Fig.5);

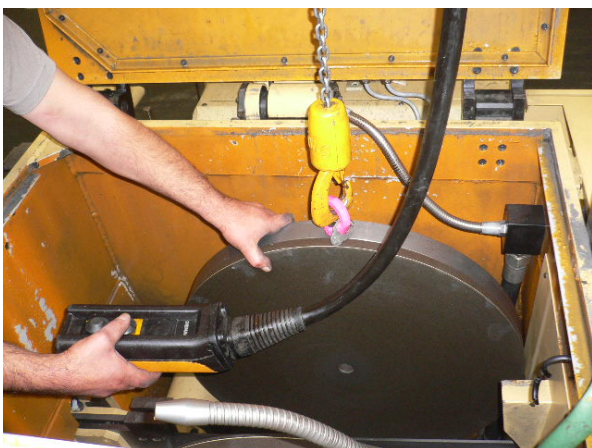


Fig.5 Penetration of the cutting fluid by the 30 mm hole in the center of the abrasive disc.

As in the case (a) the liquid supplied in this manner intervenes in the process of cutting only when the parts are in the second half of the abrasive body.

c) The nozzles are located at the entrance grinding chamber (Fig.6);

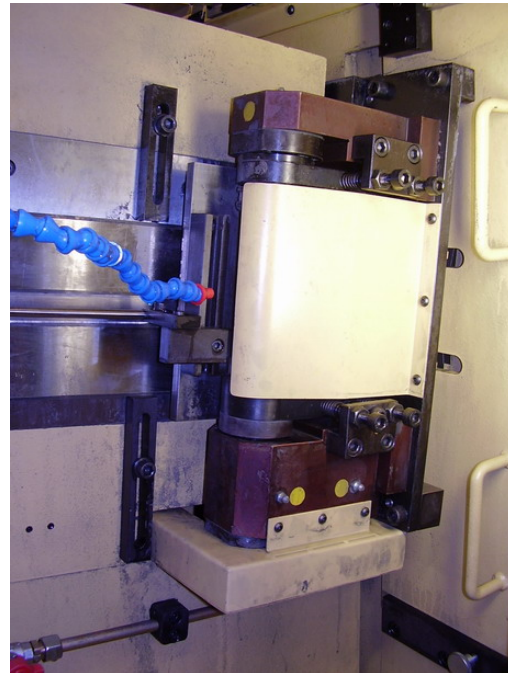


Fig. 6 Bringing the cutting fluid at the entrance of the grinding chamber.

The cutting fluid is driven to slot grinding and intervenes in the cutting process since the early removal of the material.

d) The channels or holes made in the abrasive bodies (Fig.7);

Cutting fluid brought to the cutting zone through the center bore of grinding discs stones flows through the radial channels (driven by centrifugal force) to the outside zone of the abrasive.

The grains located on the front side of the abrasive body have different rotation speeds and thus assisting in the cutting operation with variables cutting speed.



Fig.7 Channels and holes in the abrasive bodies.

Speed abrasive body is given by equation (4):

$$n_s = \frac{1000 \cdot 60}{\pi} \cdot \frac{v_s}{d_s} [\text{rot}/\text{min}] \quad (4)$$

where n_s is the speed of the abrasive body [rev / min] v_s - the peripheral speed of the abrasive body [m/s], d_s - the external diameter of the abrasive body [mm].

An abrasive grain at a distance "r" from the center of the abrasive body will have the speed v_r given by the relation (5):

$$v_r = \frac{\pi \cdot n_s \cdot 2 \cdot r}{1000 \cdot 60} [m/s] \quad (5)$$

4 Performance analysis of simultaneous flat grinding process

In experiments carried out in simultaneous flat grinding operation, the population was considered as consisting of all workpieces between two successive corrections of abrasive bodies' surfaces (around 40,000 pieces). Given the large number of the parts is not possible to measure all of them. From the population has taken a sample (subset of the population): 5 pieces each every 5000 pieces. Furthermore, roughness R_a and R_z were measured on the both side of the part's surfaces. We note with R_{amax} respectively $R_{z\text{max}}$ the highest value

obtained by measuring R and R_a respectively on one side and the other machined parts.

We can say that the information collected from the sample is representative of the population.

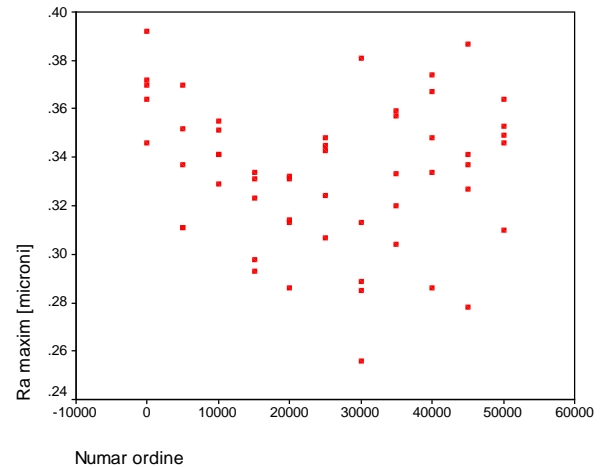


Fig.8 Values of R_{amax} taken from the both sides of parts.

By analyzing the graph in Fig.8 (Scatter the time evolution of R_{amax} roughness) R_a roughness values are found to decrease immediately after diamond dressing and then remain on a plateau. When grinding stones have been spent (by blunting the abrasive grain, binder and shoving them into the granule surface by welding a metal oxide layer) cuts through abrasive grains but not "break" the metal piece. In this way parts roughness increases rapidly.

In the grinding process, the sharp grains of the grinding wheel become rounded and hence lose their cutting ability. This condition is termed grinding wheel-glazing. Along with grain wear, another factor that reduces the cutting ability is the loading of voids between the grains with the chips and waste of the grinding process, resulting in a condition known as wheel loading. A worn and loaded wheel ceases to cut. Its cutting ability can be restored by dressing or truing.

With SPSS program regression curves were calculated for the experimental data of Fig 6. The curve that best fits the experimental data is the cube. The regression is significant at 0.05 points of significance. Its regression curve and coefficients are given in Fig.9.

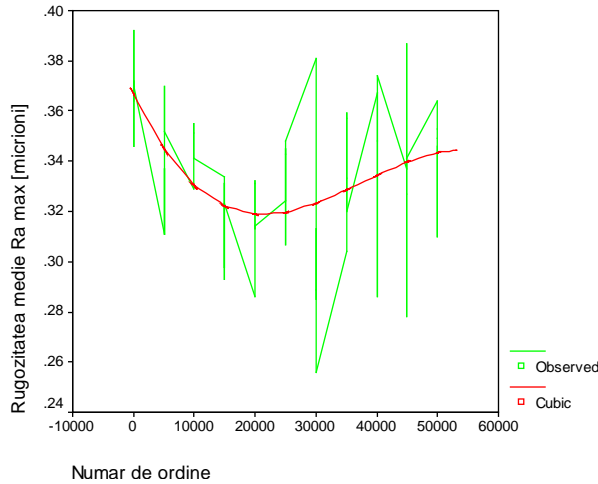


Fig.9 Regression curve of the roughness $R_{a\max}$.

The dispersion of the 55 measured values of roughness R_{\max} is shown in Fig.10. It notes that the standard deviation is 0.003 and the arithmetic mean is 0.334.

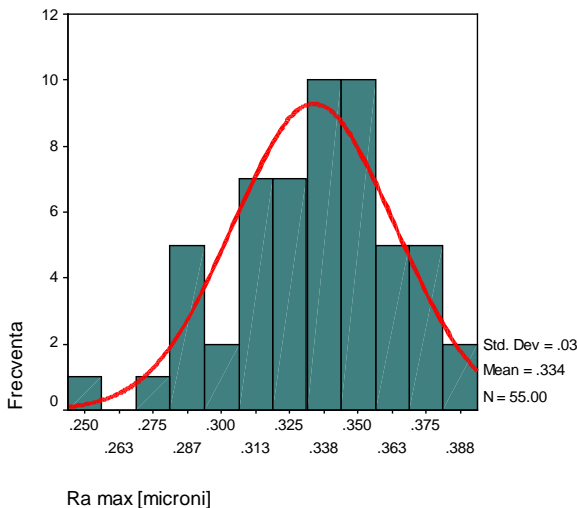


Fig.10 Dispersion of the roughness $R_{a\max}$ for parts taken from two diamond dressing.

From the analysis of the graphs in Fig.9 and Fig.10 is noted that for the study the influence of various factors on quality of grinding parts is not sufficient to measure only one piece every 5000 parts but 5 pieces repeatedly.

Of the many factors that influence on the quality of the parts, in the following we will study the influence on the quality of the machined surface, expressed by roughness R_a and R_z , of the following factors:

- Size of the machined surface size (characterized by the value OD: 17 mm, 18 mm, 19 mm (all the parts have the same internal diameter));
- The feed rate of the parts (8 m / min, 8.7 m / min 9 m / min, 11m / min);
- Abrasive grain;
- Cutting fluid;

At each step of the experiment were maintained unchanged all the above factors except one.

a) Influence of the machined surface size on the part roughness

In what follows we note with RAMIN 17 and RAMAX17 roughness R_a measured on the both sides of thye parts with OD of 17 mm. Similarly, respectively RAMAX18 RAMIN18 and roughness R_a RAMIN19 and RAMAX19 is measured on the both sides of the parts with OD of 18 mm or 19 mm.

The pieces were processed with the same cutting parameters.

In Tab.1 were represented descriptive statistics indicators for measured roughness. It notes the large number of measurements (60 for parts with OD of 17 mm and 19 mm respectively 55 parts with OD of 18 mm) to extract high degree of generality conclusions.

Tab.1 Descriptive statistics indicators for measured roughness

	N		Mean		Std. Deviation	Variance	Range	Minimum	Maximum
	Valid	Mssing	Statistic	Std. Error	Statistic	Statistic	Statistic	Statistic	Statistic
	Statistic	Statistic	Statistic	Std. Error	Statistic	Statistic	Statistic	Statistic	Statistic
RAMIN17	60	0	.27512	3.53E-03	2.73E-02	7.48E-04	.141	.226	.367
RAMAX17	60	0	.30755	4.45E-03	3.45E-02	1.19E-03	.170	.247	.417
RAMIN18	55	5	.30020	3.61E-03	2.68E-02	7.17E-04	.136	.217	.353
RAMAX18	55	5	.33385	3.98E-03	2.95E-02	8.71E-04	.136	.256	.392
RAMIN19	60	0	.29882	4.17E-03	3.23E-02	1.04E-03	.158	.214	.372
RAMAX19	60	0	.33323	4.20E-03	3.25E-02	1.06E-03	.163	.273	.436

The amplitude dispersions is between 0,136µm and 0,170µm.

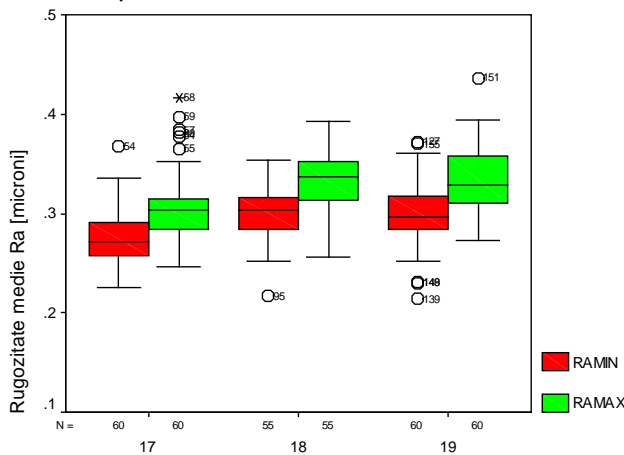


Fig.11 Box- plot Ra for parts with OD of 17, 18, 19 mm (N- number of measurements).

The standard deviation expresses that the of roughness values of R_{amin} fluctuate, on average, by more or less than 0,0273µm around average for parts with OD of 17mm, while the values of R_{amin} of the parts with OD diameter of 18 mm or 19 mm fluctuate, on average, more than 0.0268 respectively 0.0323 µm around the mean. From the analysis of the graphs in Fig.11, is found that

the parts size surfaces have not a great influence on the roughness obtained.

Analyzing the values of Tab.2 it is found that the correlation coefficients between the minimum and maximum values of roughness at flat grinding for the parts with OD of 17, 18, 19 mm are positive (between these sizes is a link directly proportional) and these link are strong (Pearson correlation coefficients are greater than 0.5). In other words, a piece that, compared to other parts of the sample has a high roughness value R_{amin} , has also a high roughness value R_{amax} .

This shows that the roughness of left and right sides depend on the size of the depth of cut.

At the same time it notes that there is no link between roughnesses of parts of different diameters.

b) Influence of the feed rate on the part roughness

The same principle was applied to the sample population: 5 pieces were taken at every 5000 machined parts. It was measured roughness R_a on one side and the other and R_{amin} and were obtained R_{amin} and R_{amax} .

Tab.2 Correlations for roughness of parts with different surface size.

		RAMAX17	RAMAX18	RAMAX19	RAMIN17	RAMIN18	RAMIN19
Pearson Correlation	RAMAX17	1.000	.032	.012	.814**	.066	-.102
	RAMAX18	.032	1.000	-.121	-.059	.649**	.029
	RAMAX19	.012	-.121	1.000	.026	-.125	.479**
	RAMIN17	.814**	-.059	.026	1.000	.064	-.167
	RAMIN18	.066	.649**	-.125	.064	1.000	-.002
	RAMIN19	-.102	.029	.479**	-.167	-.002	1.000
Sig. (2-tailed)	RAMAX17	.	.818	.929	.000	.631	.437
	RAMAX18	.818	.	.379	.668	.000	.834
	RAMAX19	.929	.379	.	.844	.364	.000
	RAMIN17	.000	.668	.844	.	.640	.202
	RAMIN18	.631	.000	.364	.640	.	.989
	RAMIN19	.437	.834	.000	.202	.989	.
N	RAMAX17	60	55	60	60	55	60
	RAMAX18	55	55	55	55	55	55
	RAMAX19	60	55	60	60	55	60
	RAMIN17	60	55	60	60	55	60
	RAMIN18	55	55	55	55	55	55
	RAMIN19	60	55	60	60	55	60

** . Correlation is significant at the 0.01 level (2-tailed).

Tab.3 Statistics of the influence of the feed rate on the roughness.

	N		Mean		Median	Std. Deviation	Variance	Range	Minimum	Maximum
	Valid	Missing	Statistic	Std. Error	Statistic	Statistic	Statistic	Statistic	Statistic	Statistic
	Statistic	Statistic	Statistic	Std. Error	Statistic	Statistic	Statistic	Statistic	Statistic	Statistic
RAMNB.1	35	70	.29569	6.98E-03	.29600	4.13E-02	1.70E-03	.178	.212	.390
RAMAX8.1	35	70	.33146	7.66E-03	.32800	4.53E-02	2.06E-03	.184	.242	.426
RAMNB.7	30	75	.26010	5.77E-03	.25700	3.16E-02	9.99E-04	.138	.179	.317
RAMAX8.7	30	75	.28950	6.24E-03	.28450	3.42E-02	1.17E-03	.144	.211	.355
RAMN9	40	65	.32860	8.03E-03	.32900	5.08E-02	2.58E-03	.213	.226	.439
RAMAX9	40	65	.36645	9.43E-03	.36400	5.97E-02	3.56E-03	.214	.253	.467

Again we see that there is a strong correlation between R_{amin} and R_{amax} roughness (between surface roughness obtained for the both sides of the piece). In other words, if the surface roughness is increased on one side means that increases the roughness on the other. This means that the machining allowance is removed uniformly from both sides, and that the wear of two abrasive discs is the same.

It also notes that there is no correlation between the roughness of the parts machined at different speeds.

As expected, increasing of the feed rate, resulted in some increase of roughness R_a , and to increase of spreading of values obtained.

From the analysis of dispersions in Fig.10, is observed that the greatest width is for the "box" roughness obtained for pieces of 19 mm outer diameter.

It can be observed the great number of measurements 35, 30 and 40, to obtain information with a high degree of certainty

Tab.4 Correlations of the influence of the feed rate on the roughness.

		RAMIN8.1	RAMAX8.1	RAMIN8.7	RAMAX8.7	RAMIN9	RAMAX9
Pearson Correlation	RAMIN8.1	1.000	.825**	.a	.a	.072	.054
	RAMAX8.1	.825**	1.000	.a	.a	.155	.125
	RAMIN8.7	.a	.a	1.000	.862**	.a	.a
	RAMAX8.7	.a	.a	.862**	1.000	.a	.a
	RAMIN9	.072	.155	.a	.a	1.000	.865**
	RAMAX9	.054	.125	.a	.a	.865**	1.000
Sig. (2-tailed)	RAMIN8.1	.	.000	.	.	.682	.757
	RAMAX8.1	.000373	.476
	RAMIN8.7000	.	.
	RAMAX8.7	.	.	.000	.	.	.
	RAMIN9	.682	.373000
	RAMAX9	.757	.476	.	.	.000	.
N	RAMIN8.1	35	35	0	0	35	35
	RAMAX8.1	35	35	0	0	35	35
	RAMIN8.7	0	0	30	30	0	0
	RAMAX8.7	0	0	30	30	0	0
	RAMIN9	35	35	0	0	40	40
	RAMAX9	35	35	0	0	40	40

** . Correlation is significant at the 0.01 level (2-tailed).

a. Cannot be computed because at least one of the variables is constant.

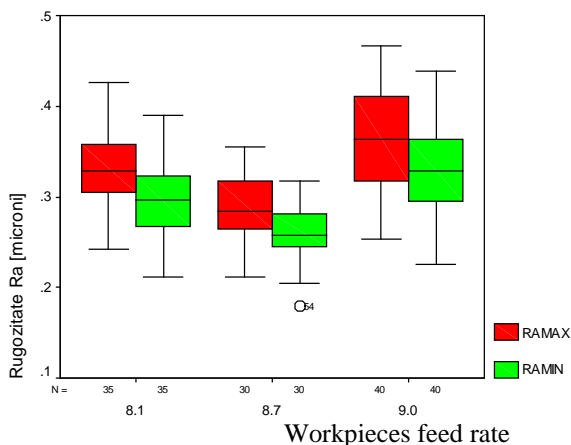


Fig.12 Box-plot R_a according with feed rate of workpieces.

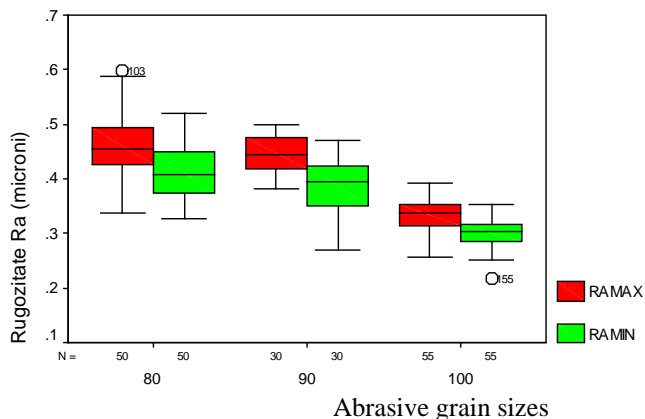


Fig.13 Box plots R_{amax} and R_{amin} according with abrasive grain sizes, (N- number of measurements).

c) Influence of abrasive grains on the parts roughness

In Fig.13 and Fig.14 are represented Box plots of roughness R_a and R_z for pieces of different abrasive grain sizes.

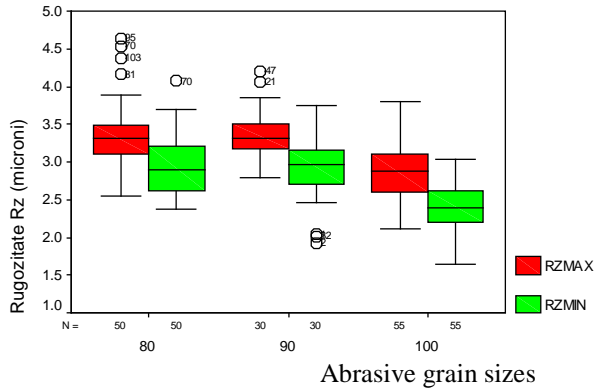


Fig.14 Box- plots R_{zmax} and R_{zmin} according with abrasive grain sizes, (N- number of measurements).

From Fig.13 and Fig.14, it appears that as the abrasive grain is finer surface roughness Ra is smaller.

d) Influence of the cutting fluid on the part roughness

Cutting fluid is provided by a centralized cutting fluid system. The parameters of cutting fluid are monitored and corrected in the shortest time. This means that during the operation of the central system was not observed large changes of the characteristic parameters of the emulsion (concentration, the tendency of foaming, pH, content of impurities and foreign oil).

Roughness R_a and R_z were measured for of the parts before and after the emulsion changing and their results are shown in Fig.15 and Fig.16 (after machined 5,000 workpieces were measured 5 of them).

After analysing of Box- plots graphs results that the quality of parts machined with damaged emulsion and those machined with fresh emulsion there is variation, but this difference is not very large.

Wear wheel is not changed. Do not change the number of machined parts between two successive diamond dressing of abrasive discs. This can be explained by the fact that, even if damaged, the old emulsion had properties similar to those of the fresh emulsion, due to a suitable technology management. Stability grinding process is also very high.

The cutting is carried out within safety limits on the machine and the grinding stone. This suggests that not yet exhausted the possibilities of optimizing the grinding process.

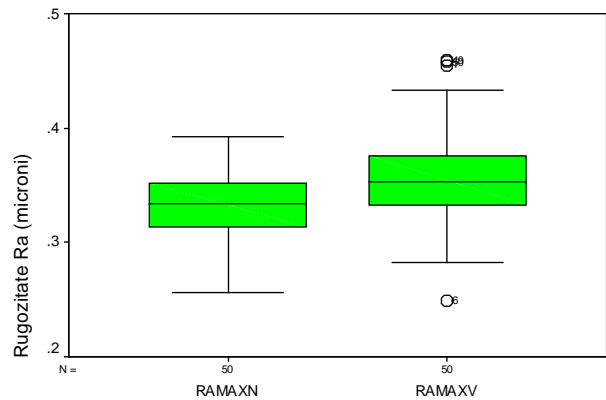


Fig.15 Box- plot R_{amax} for old and new emulsion.

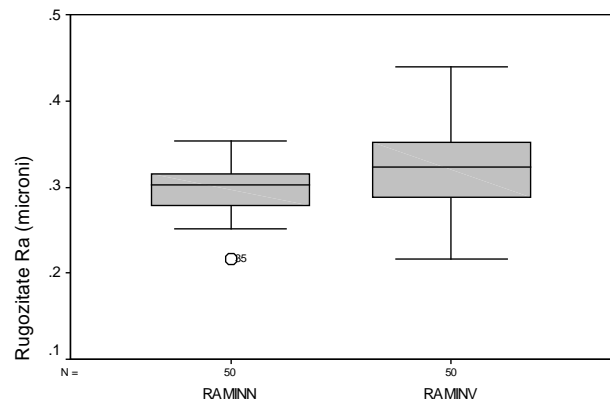


Fig.16 Box- plot R_{amin} for old and new emulsion.

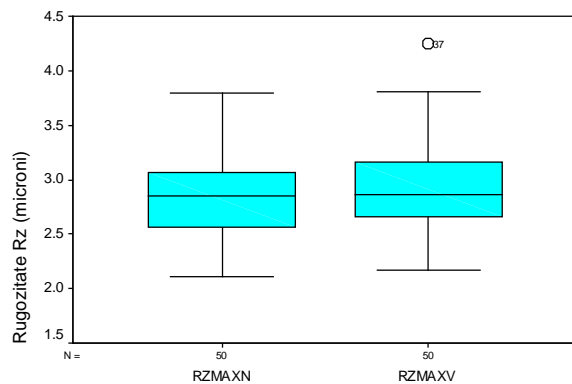


Fig.17 Box- plot R_{zmax} for old and new emulsion.

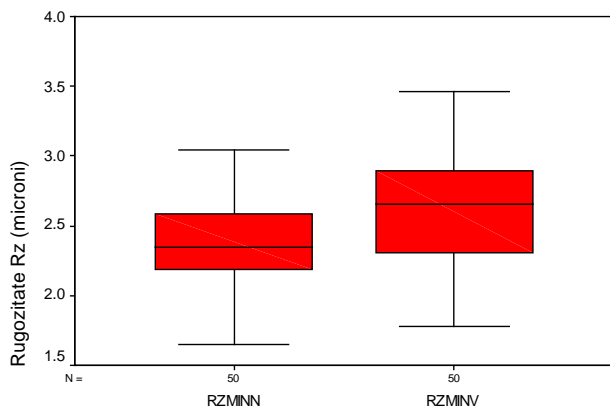


Fig.18 Box- plot R_{zmin} for old and new emulsion.

4 Conclusion

During grinding process a great percentage of energy used to remove material from the part surface is change into heat which is taken away by the chips. But because part being ground takes a range of temperature which affects the surface finish and dimensional accuracy is important to use a suitable cutting fluid which maintains removal of material in equal percentage from the entire part surface. In this way is obtained a good thermal balance which give conditions for reducing the magnitude and type of residual stresses developed. The cutting fluid may be applied on the part surface as a stream or as mist around the periphery of the wheel and in some cases from the inside of the wheel that ensure a better cooling at tool part surface.

The size of the machined surface, characterized by external diameter: 17mm, 18mm, 19mm has no great influence on the surface roughness R_{amin} and R_{amax} for the part machine by flat surface grinding. The same for the influence of feed rate.

The quality of cutting liquid has no great influence on the surface roughness obtained due to the good management of the liquid composition and of stability of technological system.

References:

- [1] A. Balacescu, C. Buzatu, *A new theoretical model of a grinding process*, RECENT magazine, vol.5, 2004.
- [2] C. Buzatu, A. Nedelcu, I. Piukovici, B. Lepadatescu, *Finishing machining processe*, LUX LIBRIS Publishing House, Brasov, 1998.
- [3] C. Buzatu, *Contributions to study about the factors which affect the part accuracy at turning and grinding*, Doctoral thesis, Transilvania University of Brasov, 1981.
- [4] B. Lepadatescu, *Superfinishing of metal surfaces*, Transilvania University of Brasov Publishing House, 2004.
- [5] P. Lazar, *Contributions to establish the grinding wheel grade*

Creative Commons Attribution License 4.0 (Attribution 4.0 International, CC BY 4.0)

This article is published under the terms of the Creative Commons Attribution License 4.0

https://creativecommons.org/licenses/by/4.0/deed.en_US